Numerical continuation of standing waves for the Davey-Stewartson equation

Teo Nilsson

Master's thesis
2016:E14

Lund University

Faculty of Science
Centre for Mathematical Sciences
Mathematics

Centrum Scientiarum Mathematicarum

Abstract

This thesis considers solitary standing wave solutions to the Davey-Stewartson equation, which is a model for surface waves on a body of water in three dimensions. In a special case, the Davey-Stewartson equation is reduced to the well-known non-linear Schrödinger equation with cubic power which is known to have a countable familiy of radial standing waves. One of the aims of this thesis is to investigate whether this also is the case for the Davey-Stewartson equation by considering the linearization around these radial solutions. In particular, for the ground state it can be shown that the kernel is empty if we restrict the equation to even functions. We numerically investigate if the same is true for the excited states. Also, numerical continuation and bifurcation detection is done using the radial solutions as initial values.

Acknowledgements

I sincerely thank my supervisor Erik Wahlén for his valuable input, extensive expertise and whom without this thesis never would have been possible to complete. My graditude extends to friends, family and loved ones for their continuous support. A special thanks is dedicated to Anna-Maria Persson who never stopped being a mentor.

Contents

1 Introduction **1**

2 The non-linear Schrödinger equation **3**
2.1 Restriction to even functions 7

3 The Davey-Stewartson equation **8**
3.1 Domain of parameters 8
3.2 Linearization around non-radial solutions 11

4 Numerical methods **15**
4.1 Numerical continuation 15
4.2 Iterative methods 17

5 Results **19**
5.1 Ground state 20
5.2 First excited state 23
5.3 Second excited state 25
5.4 Negative delta 27

6 Summary and discussion **30**

Appendix **31**

A Mathematical framework **31**
A.1 Lebesgue and Sobolev spaces 31
A.2 The Fourier transform 33
A.3 Operator theory 34

Bibliography **38**

1 Introduction

The Davey-Stewartson (DS) equation[1]

$$iA_t + a_1 A_{xx} + a_2 A_{yy} = -a_3|A|^2 A - a_4 \phi_x A,$$
$$b_1 \phi_{xx} + \phi_{yy} = b_2(|A|^2)_x,$$

where $A = A(x, y, t)$ and $\phi = \phi(x, y, t)$ are the (complex) wave-amplitude and (real) mean velocity potential, was derived in 1974 by A. Davey and K. Stewartson [7] as a model for weakly non-linear surface waves in the form of wave packets on a body of water of finite depth. In fact, the same equation appeared already in the paper [3] from 1969 by Benney and Roskes. Djordjevic and Redekopp [8] extended the model to include surface tension effects. In Cartesian coordinates, the water surface is described asymptotically by

$$z = \varepsilon \left(iAe^{i(kx-\Omega t)} - i\bar{A}e^{-i(kx-\Omega t)} \right) + O(\varepsilon^2),$$

where $A = A(\varepsilon(x - c_g t), \varepsilon y, \varepsilon^2 t)$ and $0 < \varepsilon \ll 1$. Here k is the wave number of the background wave train which is modulated by the envelope A, Ω the angular frequency and $c_g = \partial\Omega/\partial k$ the corresponding group speed. Formulas for the coefficients a_1, a_2, a_3, a_4 and b_1, b_2 in terms of physical quantities can be found in [8]. In particular, it can be shown that

$$a_2, a_4, b_2 \geq 0,$$

whereas the other coefficients have arbitrary signs. In what follows, we will however take a more general approach and only assume that

$$a_1, a_2, a_3, b_1, b_2 \neq 0.$$

In this thesis, we look for solitary standing wave solutions of the Davey-Stewartson equation of the form $A(x, y, t) = e^{i\omega t}\psi(x, y)$ and $\phi = \phi(x, y)$ with

[1] We will use the term 'equation' throughout the thesis, although it can of course also be seen as a system of two equations. Later on we will rewrite the system as a single, scalar, non-local equation.

$\psi(x,y), \phi(x,y) \to 0$ as $|(x,y)| \to \infty$. This gives the equations

$$a_1\psi_{xx} + a_2\psi_{yy} - \omega\psi = -a_3|\psi|^2\psi - a_4\phi_x\psi,$$
$$b_1\phi_{xx} + \phi_{yy} = b_2(|\psi|^2)_x.$$

Rescaling x, y, ψ and ϕ one can transform this into

$$\epsilon\psi_{xx} + \psi_{yy} - \omega\psi = -\delta|\psi|^2\psi - \gamma\phi_x\psi, \tag{1.1}$$
$$\phi_{xx} + \rho\phi_{yy} = (|\psi|^2)_x, \tag{1.2}$$

where $\epsilon = \pm 1$, $\delta = \pm 1$, $\omega = \pm 1$ and $\gamma \in \mathbb{R}$ and $\rho \in \mathbb{R}$ are arbitrary. When $\epsilon = 1$ and $\rho > 0$, the Davey-Stewartson equation (1.1)–(1.2) is called elliptic-elliptic. This is the case which will be considered throughout the thesis. In addition, we will assume that $\omega = 1$ and in most of the thesis we will also assume that $\delta = 1$. The restriction $\omega = 1$ can be shown to be necessary for the existence of solitary standing waves by similar considerations as in section 3.1; see e.g. [9]. Under these assumptions, letting $\gamma = 0$ reduces equation (1.1) to the well-known focusing cubic non-linear Schrödinger (NLS) equation

$$\psi_{xx} + \psi_{yy} - \psi = -|\psi|^2\psi. \tag{1.3}$$

The physical interpretation of having $\gamma \to 0$ in the surface-wave model is that the depth of the fluid tends to infinity [8].

2 The non-linear Schrödinger equation

Consider the stationary two-dimensional cubic NLS equation

$$\psi_{xx} + \psi_{yy} - \psi = -|\psi|^2\psi \tag{2.1}$$

where $\psi : \mathbb{R}^2 \to \mathbb{C}$. In this thesis, focus will be given to radial solutions of the form

$$\psi = Q(r),\ Q : [0, \infty) \to \mathbb{R} \tag{2.2}$$

where $Q(r) \to 0$ as $r \to \infty$. These are not the only solutions to the NLS equation however. Solutions of the form $\psi = Q(r)e^{im\theta}$, $m \in \mathbb{Z}$ have been obtained by Lions and Iaia & Warchall, see [16] and [11]. From now on we consider real-valued solutions, in which case equation (2.1) reduces to

$$-\Delta\psi + \psi - \psi^3 = 0. \tag{2.3}$$

Equation (2.3) is known to have countably many radial solutions $\{\psi_n\}_{n=0}^{\infty}$, each with exactly n number of roots as a function of $|x|$, see for example [12] and [17]. The solutions are smooth and decay exponentially to zero together with all their derivatives as $|x| \to \infty$. In particular, the solution without roots, ψ_0, is often referred to as the ground state. This solution is a decreasing positive function of $|x|$ which tends to 0 as $|x|$ goes to infinity. The radial solutions ψ_n with $n \geq 1$ are known as excited states. The uniqueness of the ground state was proved by Kwong [15] and the uniqueness of the excited states was until recently an open question, but finally proved by Cortázar et al. [6].

In the remainder of this chapter, we assume that ψ_* is one of the known radial solutions $\{\psi_n\}_{n=0}^{\infty}$ to the NLS equation discussed in this chapter. Our interest is the Fréchet derivative of the left hand side of equation (2.3) in a

radial solution ψ_*, here denoted by T and obtained by considering

$$\begin{aligned}&-\Delta(\psi_*+v)+(\psi_*+v)-(\psi_*+v)^3=\\&-\Delta\psi_*+\psi_*-\psi_*^3\underbrace{-\Delta v+v-3(\psi_*)^2v}_{Tv}+R(v)\end{aligned}$$

where

$$R(v)=-3\psi_*v^2-v^3 \tag{2.4}$$

and $v\in H^2(\mathbb{R}^2)$. Since $H^2(\mathbb{R}^2)$ is an algebra (Theorem A.4) we have

$$\begin{aligned}&\|R(v)\|_{L^2(\mathbb{R}^2)}\le\|R(v)\|_{H^2(\mathbb{R}^2)}\le C\|\psi_*\|_{H^2(\mathbb{R}^2)}\|v\|^2_{H^2(\mathbb{R}^2)}+\|v\|^3_{H^2(\mathbb{R}^2)}\\&\le\tilde{C}\|v\|^2_{H^2(\mathbb{R}^2)}=\mathcal{O}(\|v\|^2_{H^2(\mathbb{R}^2)})\end{aligned}$$

as $\|v\|_{H^2}\to 0$. This shows that T is the Fréchet derivative of the right hand side of equation (2.3) if this is considered as an operator from $H^2(\mathbb{R}^2)$ to $L^2(\mathbb{R}^2)$.

The operator T can be decomposed as $T=A+B$, where $Av=v-\Delta v$ and $Bv=-3\psi_*^2v$. The operator $A=I-\Delta$ is a self-adjoint operator on $L^2(\mathbb{R}^2)$ with domain $\mathcal{D}(A)=H^2(\mathbb{R}^2)$ and it is known that

$$\sigma(I-\Delta)=\sigma_{ess}(I-\Delta)=[1,\infty); \tag{2.5}$$

see for example Hislop and Sigal [10, p.73]. Since ψ_* is real, smooth and exponentially decaying, it is clear that B is a bounded, symmetric operator on $L^2(\mathbb{R}^2)$. We show in Proposition 3.2 below that it is also relatively A-compact. It therefore follows from Theorem A.7 that T is self-adjoint on $L^2(\mathbb{R}^2)$ with domain $H^2(\mathbb{R}^2)$ and from Theorem A.8 that

$$\sigma_{ess}(T)=\sigma_{ess}(I-\Delta)=[1,\infty).$$

In particular, T can only have point spectrum below one and one can in fact show that it only has finitely many eigenvalues less than one (see Chang et al. [4]). However, the main interest for us is the eigenvalue zero. Note that,

$$T\partial_x\psi_*=-\Delta\partial_x\psi_*+\partial_x\psi_*-3(\psi_*)^2\partial_x\psi_*=\partial_x(-\Delta\psi_*+\psi_*-\psi_*^3)=0$$

and the symmetry in x and y yields the inclusion

$$\operatorname{span}\{\nabla\psi_*\}\subseteq\mathcal{N}(T) \tag{2.6}$$

for all radial solutions ψ_*. The following result, relying on Sturm-Liouville theory, is due to Chang et al. [4]. Here the special case of cubic non-linearity in two dimensions is discussed but a similar result holds for arbitrary powers $p>1$ and is presented with a complete proof in [4]. Note that the proof by Chang et al. also works in $\mathbb{R}^d$ for any $d\ge 1$.

Proposition 2.1 *Let ψ_0 be the unique ground state of* (2.3). *Then we have*

$$\mathcal{N}(T) = \text{span}\{\partial_x \psi_0, \partial_y \psi_0\}. \tag{2.7}$$

This proposition says that the ground state is non-degenerate, meaning that the only solutions to the linearized equation at the ground state are related to symmetries of the equation (in this case translation invariance in x and y).

Before giving the proof we state two lemmas which we will use in the proof. In the second lemma and the proof of the proposition, we use the notation $A|_V \geq 0$ to indicate that

$$\langle Av, v\rangle \geq 0$$

for all $v \in V$, where A is a self-adjoint operator on a Hilbert space X and V a closed (but not necessarily A-invariant) subspace of X. Similarly, $A|_V > 0$ means that there exists a constant $c > 0$ such that

$$\langle Av, v\rangle \geq c\|v\|^2$$

for all $v \in V$. The notation $A \geq 0$ (or $A > 0$) is used in place of $A|_X \geq 0$ (or $A|_X > 0$).

Lemma 2.2

$$T\psi_0 = -2\psi_0^3 \quad \textit{and} \quad T\tilde{\psi}_0 = -2\psi_0,$$

where

$$\tilde{\psi}_0 = (1 + x \cdot \nabla)\psi_0.$$

Proof This follows by straightforward computations.

Lemma 2.3 $T|_{\{\psi_0^3\}^\perp} \geq 0$.

Proof This follows from a variational characterization of ψ_0 and is proved in Chang et al. [4], to which we refer for details.

Proof of Proposition 2.1 Since the potential in T is radial, any solution of $Tv = 0$ can be decomposed as

$$v(r,\theta) = v_{1,1}(r) + \sum_{k\geq 1} v_{k,1}(r)\cos(k\theta) + v_{k,2}(r)\sin(k\theta) \tag{2.8}$$

where $r = |x|$ and $Tv = 0$ if and only if $A_k v_{k,j} = 0$ where $k = 0, 1, 2, \ldots$, $j = 1, 2$ (only $j = 1$ if $k = 0$) and

$$A_0 = -\partial_r^2 - \frac{1}{r}\partial_r + 1 - 3\psi_0^2(r),\ A_k = A_0 + k^2 r^{-2}.$$

The operators A_k are singular Sturm-Liouville operators on the half-line $(0,\infty)$, since they can be written in the form

$$A_k w = -\frac{1}{r}(rw')' + \left(1 - 3\psi_0^2(r) + \frac{k^2}{r^2}\right) w.$$

Each operator A_k is an unbounded self-adjoint operator on the weighted L^2 space $\{w \in L^2_{\mathrm{loc}}((0,\infty))\colon \int_0^\infty |w(r)|^2 r dr < \infty\}$. In the remainder of the proof, we will use $\langle u, v\rangle$ to denote the corresponding inner product $\int_0^\infty u(r)\overline{v(r)}rdr$. Note that there is a difference between the case $k = 0$ and the cases $k \geq 1$ in that 0 is of limit circle type for $k = 0$ and limit point type for $k \geq 1$. For these definitions and more on singular Sturm-Liouville problems we refer to Teschl [22] and Zettl [26]. What will be essential for us is that each A_k is bounded from below and has essential spectrum $[1,\infty)$, that the eigenvalues below the essential spectrum are simple and can be ordered in increasing order $\lambda_1 < \lambda_2 < \cdots$ and that an eigenfunction w_k corresponding to λ_k has exactly $k-1$ zeros on $(0,\infty)$. For these facts we refer to [26, Chapter 10].

Case 1, $k = 1$. Note that $\nabla\psi_0 = \psi_0'(r)\frac{x}{r}$. Since $A_1\psi_0' = 0$ and $\psi_0'(r) < 0$ (monotonicity of ground state) for $r \in (0,\infty)$, $\psi_0'(r)$ is the ground state of A_1 (which is unique up to multiplication by a constant). From Sturm-Liouville theory it follows that $A_1 \geq 0$ and $A_1|_{\{\psi_0'\}^\perp} > 0$.

Case 2, $k \geq 2$. Since $A_k = A_1 + (k^2-1)r^{-2}$ and $k^2 > 1$, we have $A_k > 0$ and hence $A_k v_k = 0$ has no nonzero L^2-solution.

Case 3, $k = 0$. Note that the first eigenvalue of A_0 is negative since the numerator in the Rayleigh quotient $\langle A_0\psi_0, \psi_0\rangle = \langle -2\psi_0^3, \psi_0\rangle = -2\int \psi_0^4(r) r dr < 0$. The second eigenvalue is non-negative due to Lemma 2.3, which implies that $A_0|_{\{\psi_0^3\}^\perp} \geq 0$, and the min-max principle (Theorem A.9) which implies that $\lambda_2 \geq \inf_{\psi\perp\psi_0^3} \frac{\langle A_0\psi,\psi\rangle}{\langle\psi,\psi\rangle}$. Hence, if there is a non-zero solution of $A_0 v_0 = 0$, then 0 is the second eigenvalue. By Sturm-Liouville theory, $v_0(r)$ can be taken to have only one positive zero, which we denote by $r_0 > 0$. Lemma 2.2 implies that $A_0\psi_0 = -2\psi_0^3$ and $A_0\tilde{\psi}_0 = -2\psi_0$, since ψ_0 and $\tilde{\psi}_0 = (1 + x\cdot\nabla)\psi_0$ are radial functions. Hence, we have $\langle\psi_0^3, v_0\rangle = -\frac{1}{2}\langle A_0\psi_0, v_0\rangle = -\frac{1}{2}\langle\psi_0, A_0 v_0\rangle = 0$ and $\langle\psi_0, v_0\rangle = -\frac{1}{2}\langle A_0\tilde{\psi}_0, v_0\rangle = -\frac{1}{2}\langle\tilde{\psi}_0, A_0 v_0\rangle = 0$. Let $\alpha = \psi_0^2(r_0)$. Since $\psi_0'(r) < 0$ for $r > 0$, the function $\psi_0^3 - \alpha\psi_0 = \psi_0(\psi_0^2 - \alpha)$ is positive for $r < r_0$ and negative for $r > r_0$. Thus $v_0(\psi_0^3 - \alpha\psi_0)$ does not change sign, contradicting $\langle v_0, \psi_0^3 - \alpha\psi_0\rangle = 0$.

Combining these cases proves the lemma.

2.1 Restriction to even functions

For all radial solutions of equation (2.3) we have the inclusion

$$\text{span}\{\nabla\psi_*\} \subseteq \mathcal{N}(T) \tag{2.9}$$

and in particular for the ground state ψ_0, we appeal to Proposition 2.1 which says that

$$\mathcal{N}(T) = \text{span}\{\nabla\psi_0\}. \tag{2.10}$$

The partial derivatives can be excluded from the kernel by restricting the operator to subspaces of even functions

$$H_e^2(\mathbb{R}^2) = \{\psi \in H^2(\mathbb{R}^2) : \psi(x_1, x_2) = \psi(-x_1, x_2) = \psi(x_1, -x_2) \forall x_1, x_2 \in \mathbb{R}^2\},$$
$$L_e^2(\mathbb{R}^2) = \{\psi \in L^2(\mathbb{R}^2) : \psi(x_1, x_2) = \psi(-x_1, x_2) = \psi(x_1, -x_2) \forall x_1, x_2 \in \mathbb{R}^2\}.$$

Note that the Laplacian Δ and the potential preserve eveness but that an even function has an odd derivative. So, when dealing with the ground state, we can restrict equation (2.3) to even functions and conclude that

$$\mathcal{N}(T) = \{0\}. \tag{2.11}$$

It will be assumed throughout this thesis that the excited states are non-degenerate as well, which means that the identity in equation (2.10) is assumed to hold even when ψ_* is an excited state. This assumption is verified numerically when computing the solutions.

3 The Davey-Stewartson equation

In the previous chapter we considered the special case $\gamma = 0$ of the stationary DS equation which reduced to the NLS equation. We also saw that the NLS equation has an infinite family of real-valued localized radial solutions. The main goal of the remaining chapters in this thesis is to investigate whether there is also an infinite family of localized solutions of the DS equation for $\gamma \neq 0$. We begin by reviewing known results.

A first step is to rewrite the DS equation in a form similar to the NLS equation. From now on, we restrict to real-valued solutions. Solving equation (1.2) for ϕ_x and substituting into (1.1), we obtain the equation

$$\Delta\psi - \psi = -\delta\psi^3 - \gamma L(\psi^2)\psi \tag{3.1}$$

where L is defined by

$$Lu = \mathcal{F}^{-1}\left(\frac{\xi_1^2}{\xi_1^2 + \rho\xi_2^2}\hat{u}\right). \tag{3.2}$$

Here $\mathcal{F}(u) = \hat{u}$ and $\mathcal{F}^{-1}$ denotes the Fourier transform of u and the inverse Fourier transform respectively. Note that L is a bounded operator on $H^s(\mathbb{R}^2)$ since $\frac{\xi_1^2}{\xi_1^2+\rho\xi_2^2} \in L^\infty(\mathbb{R}^2)$.

3.1 Domain of parameters

This section aims to derive conditions on the parameters δ and γ necessary for the existence of a non-trivial solitary solution ψ such that $\psi \in H^1(\mathbb{R}^2)$. We write the DS equation as

$$(I - \Delta)\psi = \delta\psi^3 + \gamma L(\psi^2)\psi \tag{3.3}$$

and note that if $\psi \in H^1(\mathbb{R}^2)$ then, according to Cipolatti [5], the right hand side of equation (3.3) belongs to $L^2(\mathbb{R}^2)$. But this gives $\psi \in H^2(\mathbb{R}^2) \Rightarrow \psi^2 \in$

$H^2(\mathbb{R}^2) \Rightarrow L(\psi^2) \in H^2(\mathbb{R}^2)$ and hence $(I-\Delta)\psi \in H^2(\mathbb{R}^2) \Rightarrow \psi \in H^4(\mathbb{R}^2)$. By repeating this argument we can conclude that $\psi \in H^s(\mathbb{R}^2) \,\forall\, 1 \leq s$.

We state the DS equation again in the form

$$\psi - \Delta\psi - \delta\psi^3 - \gamma L(\psi^2)\psi = 0 \tag{3.4}$$

and assume that the parameter ρ occuring in the operator L is strictly positive. By multiplying with ψ and doing partial integration we get

$$0 < \int_{\mathbb{R}^2} \psi^2 + |\nabla\psi|^2 dx = \int_{\mathbb{R}^2} \delta\psi^4 + \gamma L(\psi^2)\psi^2 dx \tag{3.5}$$

from which we conclude that there can not possibly exist any non-trival solutions if the right hand side of equation (3.5) is non-positive. For a real-valued ψ we have $\psi^4 = \psi^2\overline{\psi^2} \Rightarrow \int_{\mathbb{R}^2} \psi^4 dx = \int_{\mathbb{R}^2} \widehat{\psi^2}\overline{\widehat{\psi^2}} d\xi = \int_{\mathbb{R}^2} |\widehat{\psi^2}|^2 d\xi$. Therefore, applying the Fourier transform yields

$$\int_{\mathbb{R}^2} \delta|\widehat{\psi^2}|^2 + \gamma\frac{\xi_1^2}{\xi_1^2+\rho\xi_2^2}|\widehat{\psi^2}|^2 d\xi = \int_{\mathbb{R}^2} \left(\delta + \frac{\gamma\xi_1^2}{\xi_1^2+\rho\xi_2^2}\right)|\widehat{\psi^2}|^2 d\xi \tag{3.6}$$

and a necessary condition for existence of solutions is that

$$\delta + \frac{\gamma\xi_1^2}{\xi_1^2+\rho\xi_2^2} > 0 \tag{3.7}$$

for at least some ξ_1 and ξ_2. We have that

$$0 < \delta + \frac{\gamma\xi_1^2}{\xi_1^2+\rho\xi_2^2} = \frac{(\delta+\gamma)\xi_1^2 + \delta\rho\xi_2^2}{\xi_1^2+\rho\xi_2^2} \Leftrightarrow 0 < (\delta+\gamma)\xi_1^2 + \delta\rho\xi_2^2. \tag{3.8}$$

Clearly this can only hold for some ξ_1 and ξ_2 if $\delta+\gamma > 0$ or $\delta > 0$. Assume $\delta > 0$. Then $(\delta+\gamma)\xi_1^2 + \delta\rho\xi_2^2 = \delta\rho\xi_2^2 > 0$ if $\xi_1 = 0$ and $\xi_2 \neq 0$. If $\delta+\gamma > 0$, then $(\delta+\gamma)\xi_1^2 + \delta\rho\xi_2^2 = (\delta+\gamma)\xi_1^2 > 0$ if $\xi_2 = 0, \xi_1 \neq 0$.

In total, the necessary conditions for a solution are

$$\delta > 0 \text{ or } \gamma > -\delta \tag{3.9}$$

and in fact, one can show that these conditions are not only necessary but also sufficient. For example, Papanicolaou et al. [19] prove the existence of a ground state solution when $\delta, \gamma > 0$ and Cipolatti [5] assumes $\gamma > 0$ and proves the existence of a ground state solution when $\delta > -\gamma$. Recall that a ground state solution is a positive solution which goes to 0 as $|x|$ goes to infinity. Finally, Eden and Topaloglu [9] consider the more general equation

$$-\Delta v + \omega v = -\chi|v|^2 v - b\mathcal{F}^{-1}\big(\alpha(\xi_1,\xi_2)\widehat{v^2}\big)v \tag{3.10}$$

where the function α is assumed to

- be even, homogeneous of zero degree and satisfy
- $0 \leq \alpha(\xi_1, \xi_2) \leq \alpha_M \; \forall (\xi_1, \xi_2) \in \mathbb{R}^2$ and
- $\alpha_1 = \lim_{s \to \infty} \alpha(s\xi_1, \xi_2)$ and $\alpha_2 = \lim_{s \to 0^+} \alpha(s\xi_1, \xi_2)$ exist.

Equation (3.1) satisfies these conditions with $\omega = 1, \chi = -\delta, b = -\gamma, \alpha_M = 1, \alpha_1 = 1, \alpha_2 = 0$. In this setting Eden and Topaloglu show that there exists a ground state solution in $H^1(\mathbb{R}^2)$ when $\chi + \alpha_1 b < 0$ or $\chi + \alpha_2 b < 0$ and $\omega > 0$. For the Davey-Stewartson equation this shows that the conditions (3.9) are sufficient.

Furthermore, Eden and Topaloglu [9] point out that a function $\psi \in H^1(\mathbb{R}^2)$ solves equation (3.4) if and only if ψ is a critical point of the functional J defined as

$$J(\psi) = \int_{\mathbb{R}^2} \frac{\psi^2 + |\nabla \psi|^2}{2} - \left(\frac{\delta \psi^4}{4} + \gamma \frac{L(\psi^2)\psi^2}{4} \right) dx \tag{3.11}$$

which on the Fourier-side equals

$$\int_{\mathbb{R}^2} \frac{|\hat{\psi}|^2 + |\xi|^2 |\hat{\psi}|^2}{2} - \frac{1}{4} \left(\delta + \gamma \frac{\xi_1^2}{\xi_1^2 + \rho \xi_2^2} \right) |\widehat{\psi^2}|^2 d\xi. \tag{3.12}$$

The ground state solution corresponds to the critical point of J with the smallest non-zero value. Also, a solution ψ to equation (3.1) is exponentially decreasing, see Cipolatti [5].

In addition to (3.5), a solution $\psi \in H^1(\mathbb{R}^2)$ must also satisfy the Pohozaev type identity

$$2 \int_{\mathbb{R}^2} \psi^2 dx = \int_{\mathbb{R}^2} \delta |\psi|^4 + \gamma L(\psi^2)\psi^2 dx, \tag{3.13}$$

see Eden and Topaloglu [9]. Identity (3.13) is derived by considering the scalings $\psi_{a,b}(x, y) = s^a \psi(s^b x, s^b y)$ and then differentiating $J(\psi)$ along the one-parameter family defined by $s \mapsto \psi_{0,-1}$. Combining (3.5) with (3.13) one finds that

$$\int_{\mathbb{R}^2} \psi^2 dx = \int_{\mathbb{R}^2} |\nabla \psi|^2 dx. \tag{3.14}$$

Equation (3.5) and (3.14) will here be denoted as the integral identities and will be a tool for evaluating the precision of the numerical solutions in the following chapters. Specifically, identity (3.5) should be valid for all numerical solutions while the second identity (3.14) is assumed to hold approximately. The reason is that we will be solving the equation on a periodic

domain which is not invariant under the scaling used to derive equation (3.13). Therefore, the numerical value of the difference

$$\int_{\mathbb{R}^2} |\nabla\psi|^2 dx - \int_{\mathbb{R}^2} |\psi|^2 dx = \int_{\mathbb{R}^2} (|\xi|^2 - 1)|\hat{\psi}|^2 d\xi \tag{3.15}$$

will be of interest later on.

3.2 Linearization around non-radial solutions

Motivated by the results in previous section we proceed by considering equation (3.1) with $\delta = 1$. By definition, the left hand side of equation (3.1) is an element of $L^2(\mathbb{R}^2)$ if $\psi \in H^2(\mathbb{R}^2)$ and to show that this is true for the right hand side as well, we rely on Theorem A.2, the Sobolev embedding theorem, which gives the estimate

$$\begin{aligned} &\|L(\psi^2)\psi\|_{L^2(\mathbb{R}^2)} \leq C\|L(\psi^2)\|_{L^2(\mathbb{R}^2)}\|\psi\|_{L^\infty(\mathbb{R}^2)} \leq C\|L(\psi^2)\|_{L^2(\mathbb{R}^2)}\|\psi\|_{H^2(\mathbb{R}^2)} \leq \\ &\leq C\|\psi^2\|_{L^2(\mathbb{R}^2)}\|\psi\|_{H^2(\mathbb{R}^2)} \leq C\|\psi\|^3_{H^2(\mathbb{R}^2)} < \infty \end{aligned} \tag{3.16}$$

for some non-negative constant C. Since all the summands belong to $L^2(\mathbb{R}^2)$, the operator

$$G : H^2(\mathbb{R}^2) \times \mathbb{R} \to L^2(\mathbb{R}^2) \tag{3.17}$$

defined by

$$G(\psi, \gamma) = \psi - \Delta\psi - \psi^3 - \gamma L(\psi^2)\psi \tag{3.18}$$

is well-defined. Also note that G is well-defined as an operator from $H^2_e(\mathbb{R}^2)$ to $L^2_e(\mathbb{R}^2)$ since the Fourier-transform and the inverse Fourier-transform appearing in L preserve eveness and since

$$\frac{\xi_1^2}{\xi_1^2 + \rho\xi_2^2}$$

is even in ξ_1 and ξ_2. Bearing this restriction in mind we will still continue to use the notation as in equation (3.17). The NLS equation is obtained by setting $\gamma = 0$,

$$G(\psi, 0) = \psi - \Delta\psi - \psi^3 = 0 \tag{3.19}$$

for which the existence of radial solutions $\psi_n \in H^2(\mathbb{R}^2)$ is known.

To calculate the Fréchet derivative of the operator in (3.18) for an arbitrary γ, we consider

$$\gamma L(\psi^2)\psi = \gamma\mathcal{F}^{-1}\left(\frac{\xi_1^2}{\xi_1^2 + \rho\xi_2^2}\mathcal{F}(\psi^2)\right)\psi \tag{3.20}$$

appearing in the right hand side of equation (3.1). The partial Fréchet-derivative of (3.20) is derived by using linearity of the Fourier transform,

$$\gamma L((\psi+v)^2)(\psi+v) - \gamma L(\psi^2)\psi = 2\gamma L(\psi v)\psi + \gamma L(\psi^2)v + R(v)$$

where $R(v) = \mathcal{O}(\|v\|^2_{H^2(\mathbb{R}^2)})$ is given by

$$R(v) = \gamma\big(L(v^2)\psi + 2L(\psi v)v + L(v^2)v\big). \tag{3.21}$$

Merging the calculations with previous ones yields the derivative of G at ψ_* for an arbitrary γ,

$$G_\psi(\psi_*,\gamma)(v) = \underbrace{(I-\Delta)v}_{A(v)} + \underbrace{-3\psi_*^2 v - \gamma\Big(2\mathcal{F}^{-1}\Big(\frac{\xi_1^2}{\xi_1^2+\rho\xi_2^2}\mathcal{F}(\psi_* v)\Big)\psi_* + \mathcal{F}^{-1}\Big(\frac{\xi_1^2}{\xi_1^2+\rho\xi_2^2}\mathcal{F}(\psi_*^2)\Big)v\Big)}_{B(v)}.$$

We already know from chapter 2 that $A(v)$ is a self-adjoint operator on $L^2(\mathbb{R}^2)$ with domain $H^2(\mathbb{R}^2)$ and that its essential spectrum is $[1,\infty)$. In order to study the spectrum of $G_\psi(\psi_*,\gamma)$ we use the results from appendix A.

Proposition 3.1 *Suppose $f \in L^2(\mathbb{R}^2)$ and that $\{w_i\}_{i=1}^\infty$ is a bounded sequence in $H^2(\mathbb{R}^2)$. Then $\{fw_i\}_{i=1}^\infty$ has a convergent subsequence in $L^2(\mathbb{R}^2)$.*

Proof If $\Omega \subset \mathbb{R}^2$ is open and bounded, we have that $H^2(\mathbb{R}^2)$ is compactly embedded in $C(\overline{\Omega})$; see Theorem A.3. Next we observe that for all $n = 1,2,3,\ldots$ there exists an R_n such that $\|f\|_{L^2(\mathbb{R}^2\setminus B_{R_n}(0))} < 1/n$. Beginning with $n=1$ and using the compact embedding, we can extract a subsequence $\{w_{1,j}\}_{j=1}^\infty$ uniformly convergent on $B_{R_1}(0)$. In the next step we consider $n=2$ and extract a subsequence from $\{w_{1,j}\}_{j=1}^\infty$ denoted by $\{w_{2,j}\}_{j=1}^\infty$ which converges uniformly on the ball with radius R_2. Continuing this procedure creates, for each n, a subsequence uniformly convergent on $B_{R_n}(0)$ and by a diagonalization argument we extract the sequence $\{w'_j\}_{j=1}^\infty = \{w_{j,j}\}_{j=1}^\infty$ which is a subsequence of the original sequence $\{w_i\}_{i=1}^\infty$ and which converges uniformly on each $B_{R_n}(0)$ to a function $w \in C(\mathbb{R}^2)\cap L^\infty(\mathbb{R}^2)$. Moreover, $\{fw'_j\}_{j=1}^\infty$ converges in $L^2(B_{R_n}(0))$ for each n to $fw \in L^2(\mathbb{R}^2)$. Finally, since

$$\begin{aligned}\sup_j \|fw'_j\|_{L^2(\mathbb{R}^2\setminus B_{R_n}(0))} &\le \sup_j \|f\|_{L^2(\mathbb{R}^2\setminus B_{R_n}(0))}\|w'_j\|_{L^\infty(\mathbb{R}^2)} \\ &\le \frac{C}{n}\sup_j \|w'_j\|_{H^2(\mathbb{R}^2)} \to 0\end{aligned}$$

as $n\to\infty$, it follows that $fw'_j \to fw$ in $L^2(\mathbb{R}^2)$.

Proposition 3.1 implies that the multiplication operator $H^2(\mathbb{R}^2) \ni v \mapsto \psi_*^2 v \in L^2(\mathbb{R}^2)$ is compact. Then note that $\mathcal{F}^{-1}\left(\frac{\xi_1^2}{\xi_1^2+\rho\xi_2^2}\mathcal{F}(\cdot)\right)$ is bounded on $H^2(\mathbb{R}^2)$ so it follows from the proposition with $w_n = v_n$ and $f = \mathcal{F}^{-1}\left(\frac{\xi_1^2}{\xi_1^2+\rho\xi_2^2}\mathcal{F}(\psi_*^2)\right)$ that the operator $\mathcal{F}^{-1}\left(\frac{\xi_1^2}{\xi_1^2+\rho\xi_2^2}\mathcal{F}(\psi_*^2)\right)v$ is compact. Finally we can show that $H^2(\mathbb{R}^2) \ni v \mapsto \mathcal{F}^{-1}\left(\frac{\xi_1^2}{\xi_1^2+\rho\xi_2^2}\mathcal{F}(\psi_* v)\right)\psi_* \in L^2(\mathbb{R}^2)$ is a compact operator by applying Proposition 3.1 with $f = \psi_*$ and $w_n = \mathcal{F}^{-1}\left(\frac{\xi_1^2}{\xi_1^2+\rho\xi_2^2}\mathcal{F}(\psi_* v_n)\right)$. In total, we conclude that B is a compact operator from $H^2(\mathbb{R}^2)$ to $L^2(\mathbb{R}^2)$.

Proposition 3.2 *Let A be the operator above defined on $\mathcal{D}(A) = H^2(\mathbb{R}^2)$. Then, the operator $B : L^2(\mathbb{R}^2) \to L^2(\mathbb{R}^2)$ defined as above is symmetric and relatively A-compact.*

Proof The operator B is symmetric since

$$\left\langle \mathcal{F}^{-1}\left(\frac{\xi_1^2}{\xi_1^2+\rho\xi_2^2}\mathcal{F}(\psi_* v)\right)\psi_*, u\right\rangle = \left\langle \mathcal{F}^{-1}\left(\frac{\xi_1^2}{\xi_1^2+\rho\xi_2^2}\mathcal{F}(\psi_* v)\right), \psi_* u\right\rangle = \left\langle \frac{\xi_1^2}{\xi_1^2+\rho\xi_2^2}\mathcal{F}(\psi_* v), \mathcal{F}(\psi_* u)\right\rangle = \left\langle v, \mathcal{F}^{-1}\left(\frac{\xi_1^2}{\xi_1^2+\rho\xi_2^2}\mathcal{F}(\psi_*)\right)\psi_*\right\rangle.$$

Since the inclusion $\mathcal{D}(A) = H^2(\mathbb{R}^2) \subset L^2(\mathbb{R}^2) = \mathcal{D}(B)$ trivially holds it only remains to be shown that $BR_A(\lambda)$ is compact for some $\lambda \in \rho(A)$, where $R_A(\lambda)$ is the resolvent of A and $\rho(A)$ the resolvent set of A. Since $I - \Delta$ is an isometric isomorphism, it has a bounded inverse. Hence $\lambda = 0 \in \rho(A)$. It is then sufficient to show that $B(I-\Delta)^{-1}$ is a compact operator from $L^2(\mathbb{R}^2)$ to $L^2(\mathbb{R}^2)$. But this is true since B is a compact operator from $H^2(\mathbb{R}^2)$ to $L^2(\mathbb{R}^2)$ and since a composition of a bounded and a compact map is compact.

It now follows from Theorem A.7 that $G_\psi(\psi_*, \gamma)$ is self-adjoint on $L^2(\mathbb{R}^2)$ with domain $H^2(\mathbb{R}^2)$ and from Theorem A.8 that

$$\sigma_{ess}(G_\psi(\psi_*, \gamma)) = \sigma_{ess}(I - \Delta) = [1, \infty).$$

independently of γ. Recall from previous chapter that if $\gamma = 0$ we know that

$$0 \notin \sigma(G_\psi(\psi_*, 0)) \tag{3.22}$$

if ψ_* is the ground state solution. If ψ_* equals an excited state we have just shown that 0 belongs to the spectrum if and only if it is in the point spectrum. Throughout this thesis it is assumed that

$$0 \notin \sigma_p(G_\psi(\psi_*, 0)) \tag{3.23}$$

and this assumption is verified numerically when it is used. Under this assumption, all requirements of the Implicit function theorem A.6 are satisfied and we can conclude that for each excited state ψ_n, there exists an open set $\mathcal{U}_n$ around 0 and an open set $\mathcal{V}_n$ around ψ_n, such that the DS equation has a unique solution in $\mathcal{V}_n$ for each $\gamma \in \mathcal{U}_n$.

4 Numerical methods

The aim of this chapter is to find numerical solutions to the DS equation for $\gamma \neq 0$. Recall that the DS equation reduces to the NLS equation if $\gamma = 0$ and that this equation has a countable family of radial solutions. Solutions to the DS equation are then obtained by doing numerical continuation from these radial solutions. While doing so, we also compute the eigenvalues of the linearization to look for bifurcations.

4.1 Numerical continuation

Simply put, the idea behind numerical continuation is to use a known (computed) solution, say u_0, such that $F(u_0, \gamma_0) = 0$, as initial guess to compute an u_1 such that $F(u_1, \gamma_1) = 0$ where the pair (u_0, γ_0) in some sense is close to (u_1, γ_1). Obviously this requires the solution of the problem to depend continuously on the parameter in question (in this case γ).

For a more extensive motivation, we assume the following framework, which we simultaneously show that our problem fits into. Bear in mind that this only serves as an introduction and for a more rigorous approach to numerical continuation we refer to Seydel [21]. Assume that we would like to solve

$$F(u, \gamma) = 0 \tag{4.1}$$

where $F : X \times \mathbb{R} \to Y$, F is at least C^1 and that the function spaces X and Y are Hilbert spaces. Also, we assume that there exists at least one solution $(u_0, \gamma_0) = (u(\gamma_0), \gamma_0)$ to equation (4.1) such that the Jacobian $F_u(u_0, \gamma_0)$ is invertible. Then we know from the implicit function theorem that there also exists a solution $(u(\gamma), \gamma)$ to equation (4.1) if $|\gamma - \gamma_0|$ is small enough. For each given solution (u_0, γ_0) to equation (4.1) we can trace out further solutions by numerical continuation which usually yields a smooth (but unknown) curve in the (u, γ)-plane. Such a curve can be parametrized with $s \in \mathbb{R}$ as

$$\mathcal{S} = \{(u(s), \gamma(s)) : s \in \mathbb{R}\}. \tag{4.2}$$

The curve $\mathcal{S}$ is often, in this context, called a branch and the set of solutions to equation (4.1) is the union of all possible branches. Let τ_0 denote the tangent to u_0 at γ_0 along this curve and assume that it can be numerically computed. Then the following scheme can be applied to find another root of (4.1).

(1) Calculate $(u_1, \gamma_1) = (u_0, \gamma_0) + \Delta\gamma\tau_0$, where $\tau_0 = (\cdot, 1)$, and use this as initial guess in (2).

(2) Iterate (u_1^i, γ_1) until convergence using for example Newton's method. If it does not converge, decrease $\Delta\gamma$ and recalculate (1).

(3) If (2) converges, set (u_0, γ_0) to be equal to the solution obtained in (2). Choose an appropriate step-size and return to (1).

The observant reader now notices an inconsistency in the algorithm provided. Assume that a given branch forms a parabola in the (u, γ)-plane characterized by having $\gamma'(s) < 0$ for some s. Then an algorithm only taking steps of positive γ-direction will not work. The cure is to add another constraint making sure we find a solution in the hyperplane orthogonal to the tangent; see [21]. However, as long as our program is able to trace out the curve, we consider this extension redundant. Still, the algorithm does not explicitly tell us how to calulate the tangent vector or what iterative solver to use, and this will be discussed below.

A very useful tool to visualize a branch, or possible several branches, is to create a curve by replacing u in $\mathcal{S}$ by its norm $\|u\|$ and plot it against γ, see [21]. Such a plot is called a bifurcation diagram, or branching diagram. The branches can start and end at different γ, also branches can intersect, merge and split. Seydel [21], defines a branch point (with respect to γ) as a point γ^* such that the number of solutions (branches) to equation (4.1) differs as γ passes over γ_0.

Concerning our problem, we know that the ground state and each excited state will induce its own branch starting in $\gamma = 0$ but its further behaviour is still unknown. We also know that as long as the eigenvalues of the linearized operator are non-zero, the continuation exists and is unique. Note that the bifurcation diagram does not distinguish between two solutions if they have equal norm for a given γ.

A bifurcation can occur only if the linearized operator has an eigenvalue equal to zero for some γ. Theoretically, having an eigenvalue equal to zero would cause numerical issues but in practice we normally expect the algorithm to "jump over" such solutions. Therefore, if we for each γ during the continuation calculate and keep track of the eigenvalues close to zero we can

detect possible bifuraction points by checking if an eigenvalue passes zero. However, we should not forget that there might be numerical issues even if the Jacobian is just almost singular. Nonetheless, keeping track of the eigenvalues detects possible bifurcation and also helps us ensure that we do not accidentically switch branch in the continuation if our initial guess turns out to be unsatisfactory.

In this thesis, the numerical continuation will start in one of the countably many radial solutions satisfying equation (3.1) with $\gamma = 0$. An initial guess to such a radial solution is found with the shooting method on an interval $(\epsilon, R]$, where $0 < \epsilon, R$ and ϵ close to zero, and then translated into a two dimensional solution by rotation and linear interpolation. Also, since the solutions are exponentially decreasing, R is chosen such that the solution is approximately equal to zero outside this interval.

4.2 Iterative methods

In this thesis, the choice of iterative solver in the numerical continuation is a preconditioned Newton Conjugate Gradient (NCG) method in accordance to recomendations of Yang [25, 24] who claims that this method converges significantly faster than any other method for many non-linear wave equations. Even though speed is not our main concern it is nevertheless a desired feature. Moreover, Yang [25] notices that this method can converge for the ground state as well as for excited states, which for us is a crucial property. One of the biggest advantages of the NCG method is that it does not require construction of any matrices. However, this might be wanted anyways by the user when calculating eigenvalues related to the problem. As the name indicates, the NCG method is based on an outer and an inner loop where the outer loop is an ordinary Newtion iteration of the form

$$u_{n+1} = u_n + \mathsf{D}u_n, \tag{4.3}$$

where $\mathsf{D}u_n$ denotes the usual Newton corrector, which is iterated until the supremum of the residual is sufficently small. Conjuate Gradient refers to the inner loop which calculates the Newton update $\mathsf{D}u_n$ for each step in the outer loop. Using the notation in Yang [25] we denote by L_0 the operator for which we aim to solve the equation $L_0 u = 0$ and let $L_{1,n}$ denote the operator L_0 linearized around u_n. We then note that if u were represented by a matrix (possibly after a discretization), the Newton-update would be obtained by solving the system of equations $L_{1,n}\mathsf{D}u_n = -L_0 u_n$. However, one main advantage of the Conjugate Gradient method is that it is "matrix-free" and allows us to use spectral methods to calculate the Newton corrector.

On the downside, this algorithm is in theory guaranteed to work only if the linearization L_1 is symmetric and positive definite but according to Yang [25], the postive definiteness requirement is redundant in practice. A complete description and corresponding discussion about the preconditioned CG method is found in Yang [25] and therefore only a short description with a few highlighted details is provided here. The CG method begins by assuming no Newton correction is needed and then proceeds to iterate as follows:

- $\mathsf{D}u^{(0)} = 0$
- $R^{(0)} = -L_0 u$
- $D^{(0)} = M^{-1} R^{(0)}$
- $a^{(i)} = \frac{\langle R^{(i)}, M^{-1} R^{(i)} \rangle}{\langle D^{(i)}, L_1 D^{(i)} \rangle}$
- $\mathsf{D}u^{(i+1)} = \mathsf{D}u^{(i)} + a^{(i)} D^{(i)}$
- $R^{(i+1)} = R^{(i)} - a^{(i)} L_1 D^{(i)}$
- $b^{(i+1)} = \frac{\langle R^{(i+1)}, M^{-1} R^{(i+1)} \rangle}{\langle R^{(i)}, M^{-1} R^{(i)} \rangle}$
- $D^{(i+1)} = M^{-1} R^{(i+1)} + b^{(i+1)} D^{(i)}$

The first remark concerns the choice of preconditioner M which should be easily invertible and according to Yang [25] often taken as the linear differential part of L_0 since equation (3.1) can be rewritten as

$$\psi - (1 - \Delta)^{-1} \big(\delta\psi + \gamma L(\psi^2)\psi \big) = 0. \tag{4.4}$$

Therefore, the choice for our algorithm will be a discretization of $M = 1 - \Delta$. The second remark concerns the stopping condition for the CG method. As Yang points out, one should avoid oversolving and neither is it clear how to measure the error. Following Yang's recommendations we measure the error in the M^{-1} weighted 2-norm and stop whenever $\|R^{(i)}\|_M < \epsilon_{CG} \|R^{(0)}\|_M$ where ϵ_{CG} is taken between 10^{-1} and 10^{-3}. Thus, we choose $\epsilon_{CG} = 10^{-2}$. The final remark concerns the "matrix-free" implementation of this algorithm where the derivatives are computed on the fourier-side after transformation which is referred to as spectral differentiation. This method is known to provide high accuracy despite a relatively coarse grid. Bearing our restriction to even functions in mind, we use a fast-discrete-cosinus-transform (FDCT) instead of a full fast-discrete-fourier-transform (FDFT), see Trefethen [23].

5 Results

Due to eveness we restrict the computations to a square in the first quadrant, impose periodic boundary conditions and due to exponential decrease of the solution, we assume that the solution is approximately equal to zero outside the computational domain. Throughout this chapter, if nothing else is explicitly stated, all results are based on a grid formed by

$$\begin{aligned}(\frac{L_x}{2N},\cdots,\frac{L_x}{2N}+k\frac{L_x}{N},\cdots,\frac{(2N-1)L_x}{2N})\times\\ (\frac{L_y}{2N},\cdots,\frac{L_y}{2N}+k\frac{L_y}{N},\cdots,\frac{(2N-1)L_y}{2N})\end{aligned} \tag{5.1}$$

where $L_x = L_y = 3\pi, k = 0, 1, \cdots, N-1$ and $N = 64$. Also $\rho = \delta = 1$ if nothing else is explicitly stated. Hence, plots showing "the whole" solution to the DS equation are created by even reflections from the first quadrant. Also, recall the integral identities from previous chapters serving as measures of numerical correctness. Graphs occuring under the titles "integral identity 1" and "integral identity 2" refer to equation (3.5) and (3.14) respectively and show the absolute value of the difference of the right- and left-hand-side of these equations.

Similar results have been obtained by Akylas and Kim, see [13, 14], who did numerical continuation of the ground state but instead of an equidistant grid they mapped the whole first quadrant to a bounded domain in the first quadrant where the problem then was solved. Milewski and Yang [18] used a method similar to ours in a study of flexural-gravity waves modelled by the Davey-Stewartson equation (but with different values of the coefficients compared to [8]). These studies lack a systematic discussion of the existence of ground states and excited states and their dependence on the parameters in the equation, though.

5.1 Ground state

Figure 5.1 visualizes the radial ground state when $\gamma = 0$. When γ is increasing the radial property is lost as seen in figure 5.2. Note that figure 5.2 does not visualize the actual solution for $\gamma = 0.1$ but rather shows what happens to the solution, in particular we can see how the radial structure is replaced by a peak shaped as an eight. In figure 5.3 we see how the solution and the norm decreases as γ increases. The integral identities are seen in the bottom subfigures of figure 5.3. The first integral identity which is expected to be equal to zero, is satisfyingly small in magnitude, with a sudden peak at $\gamma \approx 150$. Note that occasionally the error reaches machine epsilon $\approx 10^{-16}$ and can not be visualized in a logarithmic plot, hence the "gaps" in the graph. The second integral identity is a measure of the incorrectness caused by the use of a bounded domain with periodic boundary conditions, expected to be approximately equal to zero, and is visualized in the bottom right subplot in figure 5.3. The error is small for $\gamma = 0$ with a sudden increase thereafter. Still it is many orders less than the norm of the solution ψ.

The point spectrum of the ground state consists only of two isolated eigenvalues which are visualized in figure 5.4. Even though the spectrum of the discretization consists of a point spectrum only, it is here after assumed that all eigenvalues greater than or equal to one belong to the essential spectrum of the operator that was discretized. Interesting to notice is that no bifurcation happens, and the eigenvalues seem to converge to non-zero values as γ increases and the L^2-norm of the solutions seem to tend to zero.

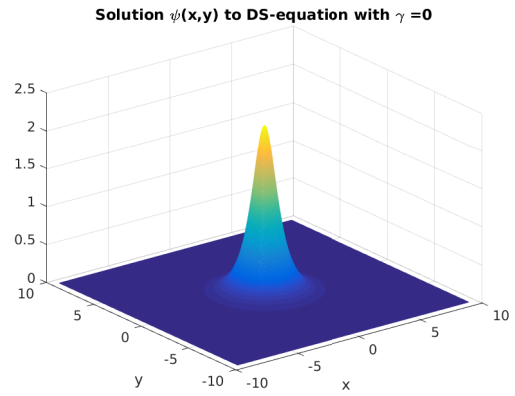

Figure 5.1: Ground state solution when $\gamma = 0$ computed with $N = 256$.

When calculating a ground state solution for negative γ we need a larger domain to preserve numerical accuracy. The reason is that the solution tends

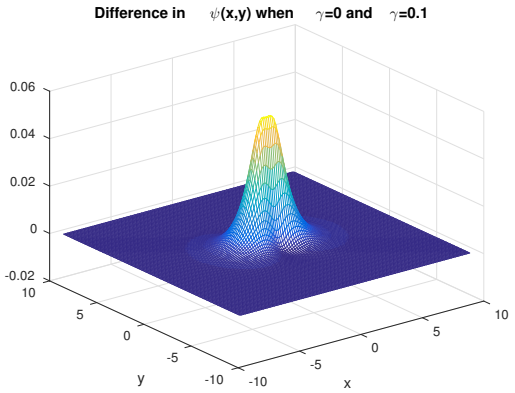

Figure 5.2: Difference between gound state solutions when $\gamma = 0$ and $\gamma = 0.1$.

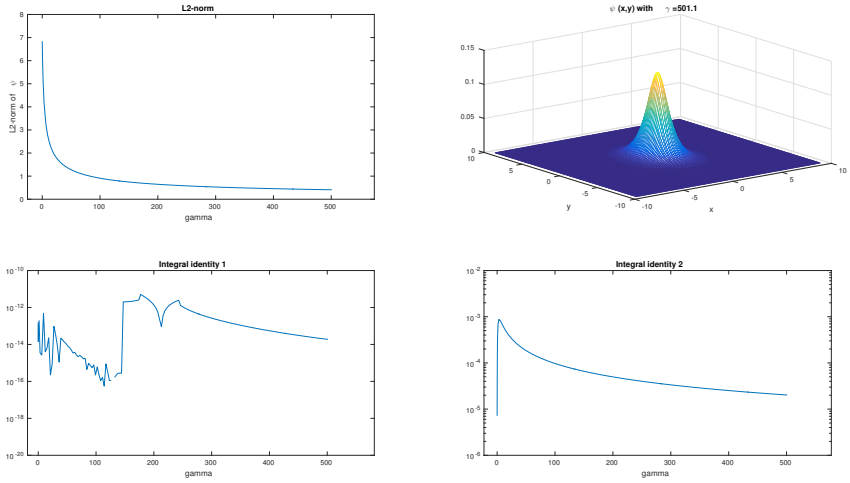

Figure 5.3: Numerical continuation of the ground state for $\gamma \in [0, 500]$.

to grow along the x-axis as seen in figure 5.5, here a grid with $Lx = 10\pi$ and $N = 128$ is used. As γ decreases the error in the second integral identity grows, most likely since the norm increases, because as figure 5.6 shows the domain seems to be suffciently large. However, if we would continue to use $N = 64$, the error in the second integral identity would approach a value of 10 when γ tends to -5.

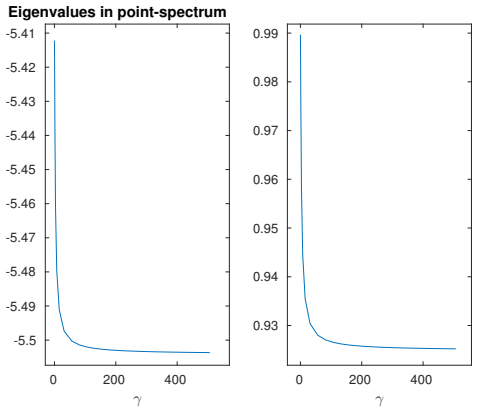

Figure 5.4: Eigenvalues of the ground state solution for $\gamma \in [0, 500]$.

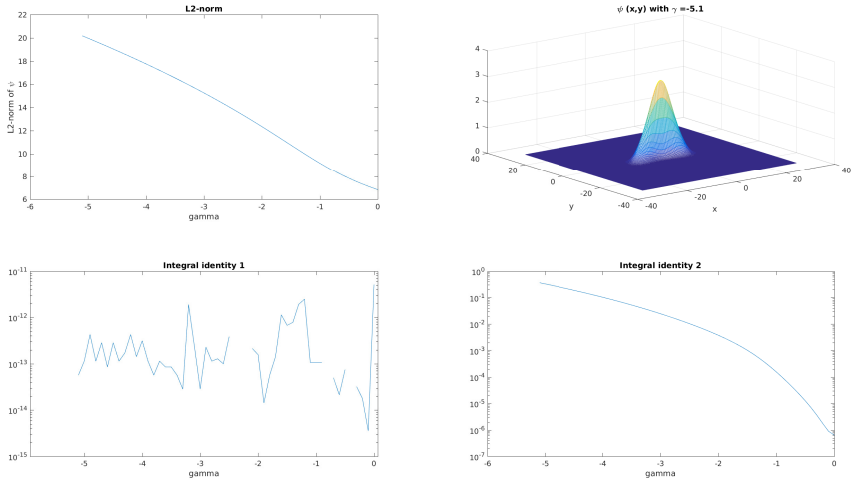

Figure 5.5: Numerical continuation of the ground state for $\gamma \in [-5, 0]$.

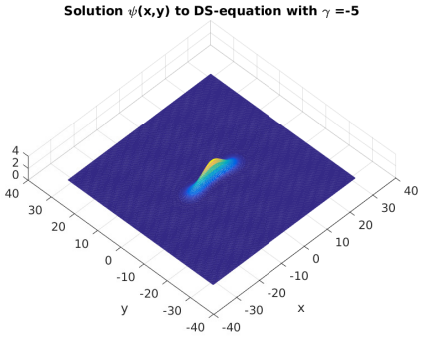

Figure 5.6: Ground state solution from above with $\gamma = -5$.

5.2 First excited state

Figure 5.7 visualizes the first excited solution to the DS equation. It is radial since $\gamma = 0$ and is the initial solution to the numerical continuation with result collected in figure 5.8.

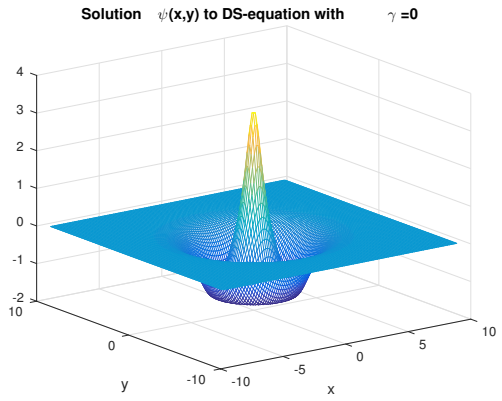

Figure 5.7: First excited state when $\gamma = 0$.

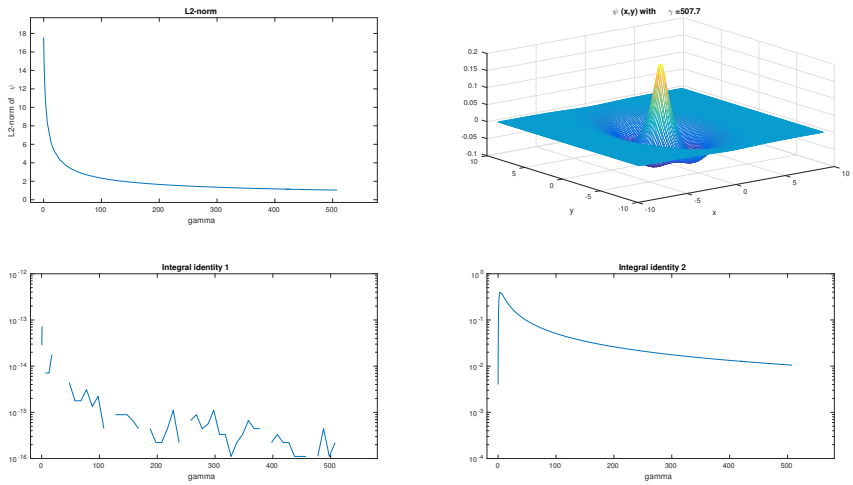

Figure 5.8: Numerical continuation with $\gamma \in [0, 500]$.

No bifurcation is detected and the smallest positive and smallest negative eigenvalues from the point spectrum of the first excited state are visualized in figure 5.9. We can also notice vague oscillations which seem to appear on what otherwise would approximately be elliptic level curves centered in the

origin. This phenomena reappear and is more visible in the second excited state.

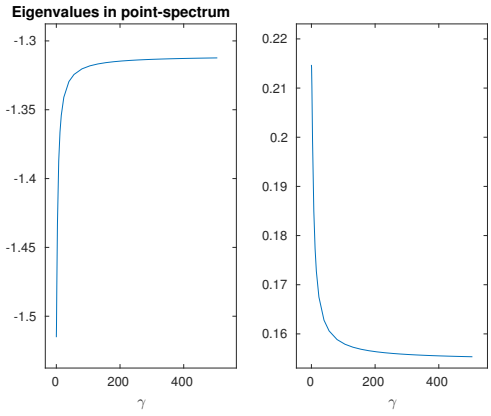

Figure 5.9: Two eigenvalues of the first excited state for $\gamma \in [0, 500]$.

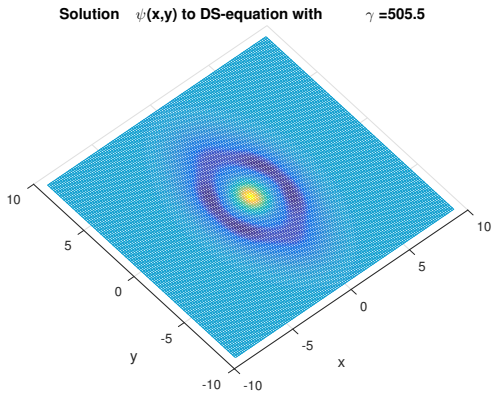

Figure 5.10: First excited state for $\gamma = 500$ seen from above.

When considering negative gamma, figure 5.11 and 5.12 show that the norm increases drastically when γ is decreasing. Compared to the ground state, the solution spreads along the x-axis much faster which induces the larger norm but also a large error in the second integral identity. When seen from above, we note that the solution spreads along the y-axis as γ tends to infinty but along the x-axis as γ decreases.

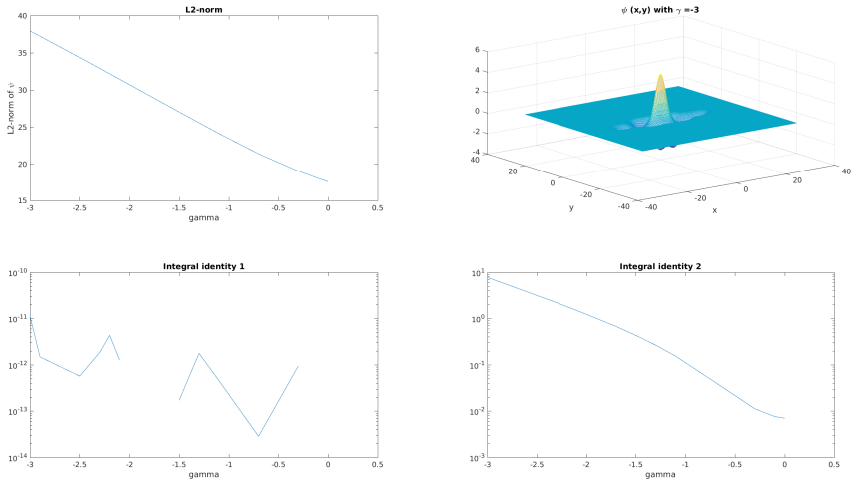

Figure 5.11: Numerical continuation with $\gamma \in [-3, 0]$.

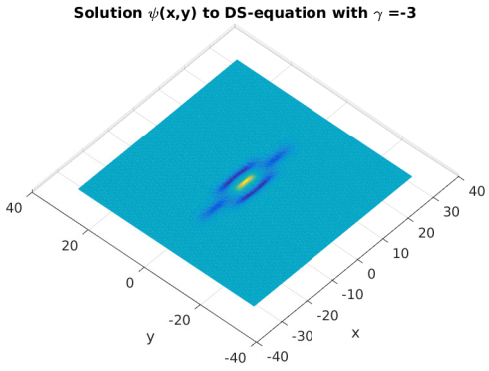

Figure 5.12: First excited state viewed from above with $\gamma = -3$.

5.3 Second excited state

When calculating the second excited state we need to enlarge the domain by using $Lx = 5\pi$. The result is found in figure 5.13. Figure 5.14 shows the largest negative and smallest positive eigenvalue, both converging as previously. Once again, the norm increases rapidly for negative γ resulting in a loss of accuracy while the solution spreads as an ellipse along the x-axis. For the calculations with $\gamma < 0$, $Lx = 7\pi$ and $N = 128$ were used. In both cases the oscillations mentioned in the previous section are amplified.

Finaly we consider the functional in equation (3.11) where the solutions to the DS equation correspond to critical points. As expected, the value of

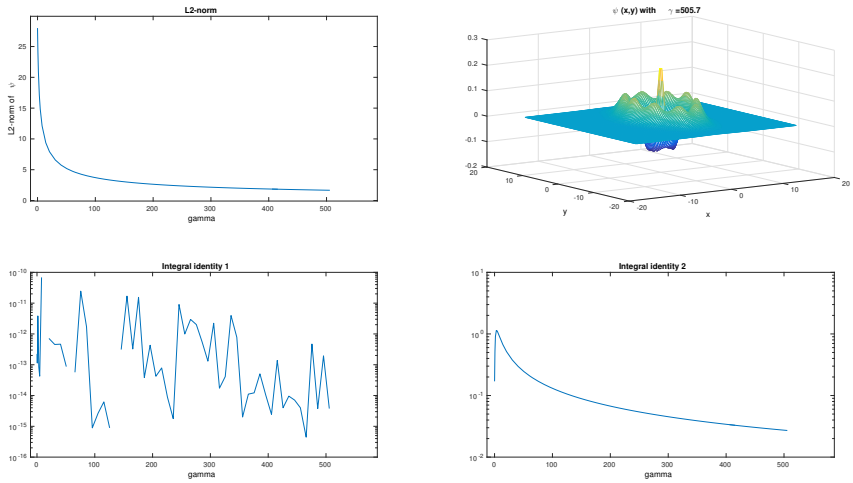

Figure 5.13: Numerical continuation with $\gamma \in [0, 500]$.

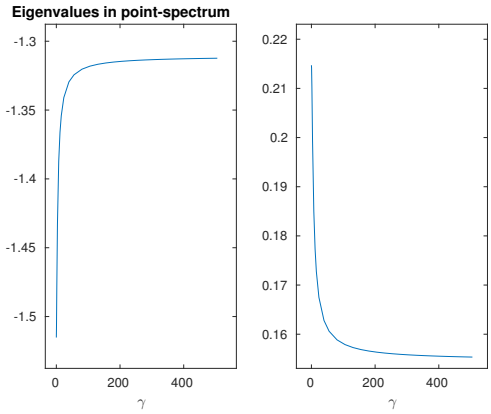

Figure 5.14: Two eigenvalues of the second excited state for $\gamma \in [0, 500]$.

the functional visualized in figure 5.16 is lower for the ground state solutions than the excited solutions.

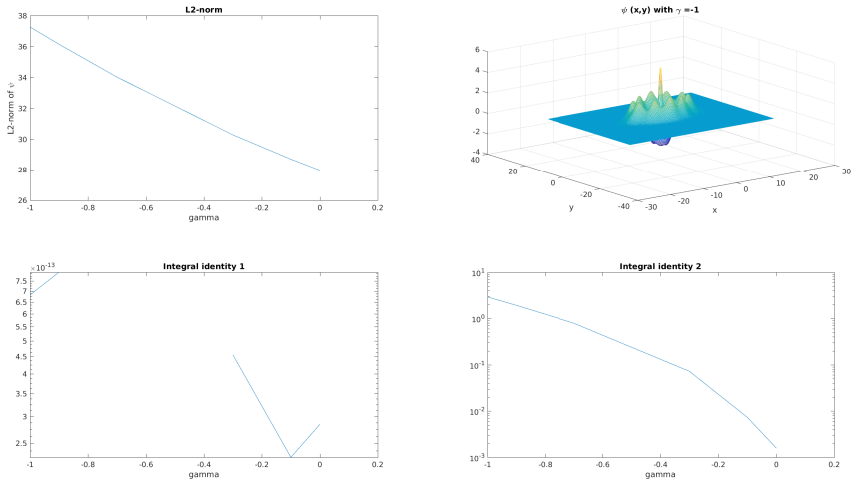

Figure 5.15: Numerical continuation with $\gamma \in [-1, 0]$.

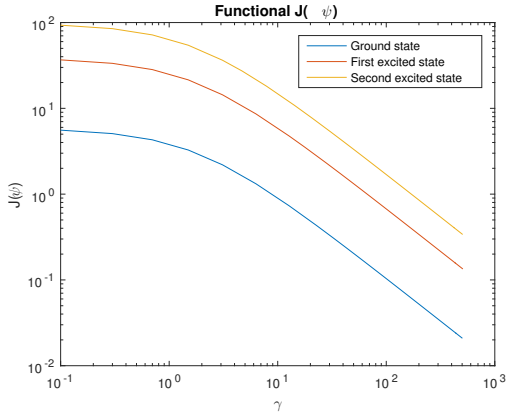

Figure 5.16: Value of the functional $J(\psi)$ for different solutions.

5.4 Negative delta

This section investigates how the ground state is affected by letting the parameter δ become negative. We recall from previous chapters that if $\delta < 0$ then $\gamma > -\delta$ is a necessary and sufficient condition for existence of a ground state solution and it is therefore natural to investigate what happens when $\gamma \to -\delta$ from above. In this section a mesh with $Lx = Ly = 10\pi$ is used and $N = 128$ except when calculating the eigenvalue where $N = 64$ where used, but the only argument for using $N = 128$ is that it provides a smaller error in the second integral identity. Figure 5.17 shows the ground state solution

for γ close to $-\delta$ and the visible peak reminds us of the peak occuring when $\delta = 1$ and $\gamma < 0$ in previous section, except for a rotation by ninety degrees. But when comparing norms, the solution in figure 5.17 is larger than for negative γ. Figure 5.18 shows how the eigenvalue in the point spectrum closest to zero seems to approach zero as γ tends to $-\delta$ but the uncertainty is high since the second integral identity is far from satisfied and the size of the computational domain seems to be insufficent. However, trying to continue the numerical continuation beyond $-\delta$ results in the trivial solution $\psi \equiv 0$ which is interesting since the norm seems to tend to infinity as $\gamma \to -\delta^+$. Figure 5.19 shows a similar result as figure 5.17 but for $\delta = -1$ and this is expected since we can always rescale the problem to get $\delta = -1$ if $\delta < 0$.

An issue with the numerical continuation when $\delta < 0$ is the lack of an initial solution. It turned out that the solutions corresponding to $\delta = -0.1$, $\gamma = 1$ and $\delta = -1$, $\gamma = 3$ were approximately radial with L2-norms between 0 and 10 which gave convergence in the Newton CG algorithm. For negative δ with a larger magnitude one is, considering the decrease of the L2-norms, probably forced to do the continuation on an unnecessary large interval unless some other trick is used. For example, one could keep γ fixed and use δ as continuation parameter.

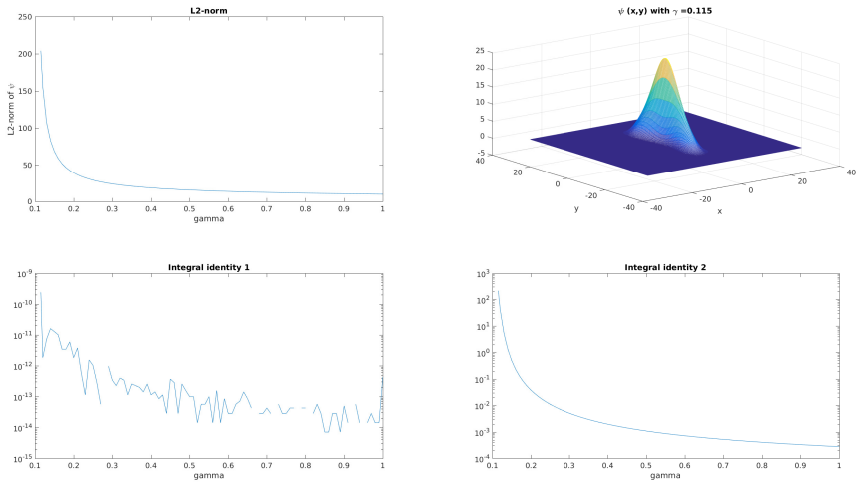

Figure 5.17: Numerical continuation with $\delta = -0.1$ and $\gamma \in [0.115, 1]$.

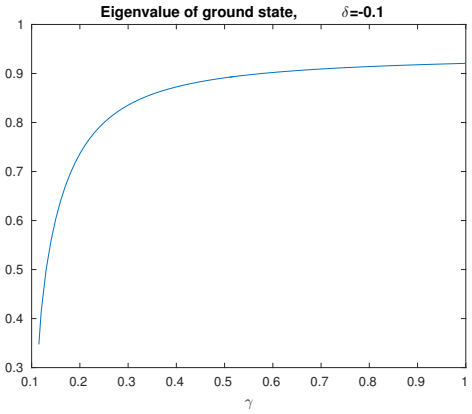

Figure 5.18: Eigenvalue when $\delta = -0.1$ $\gamma \in [0.115, 1]$.

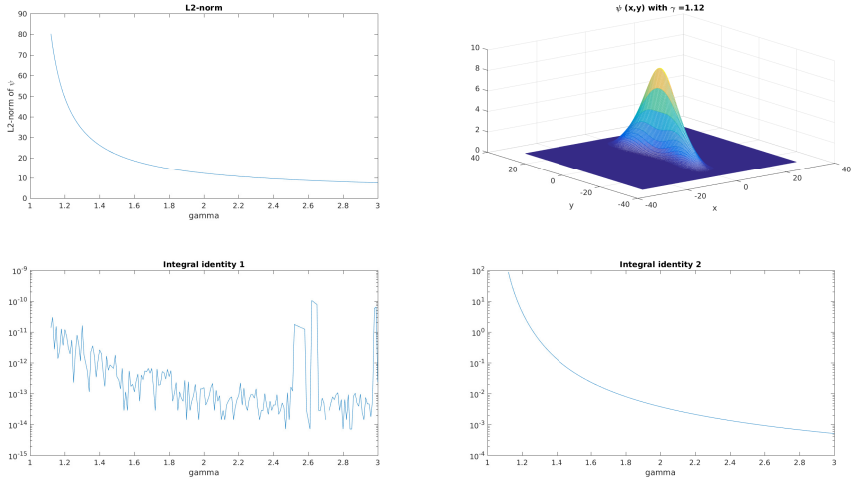

Figure 5.19: Numerical continuation with $\delta = -1$ and $\gamma \in [1.13, 3]$.

6 Summary and discussion

In summary, we have successfully applied the implicit function theorem to the radial solutions of the DS equation and concluded that there exist solutions when γ is sufficiently close to zero. The numerical results show that for positive γ the numerical continuation runs smoothly in the sense that it provides accurate results without any struggles. This is probably because we are able to solve the DS equation for the radial solution with high accuracy when $\gamma = 0$ and then the norm decreases as $\gamma \to \infty$. Still, for the excited states, the Newton CG algorithm converges slower and a larger domain is needed due to the higher variation, and larger L^2-norm, of the solution. No bifurcations were found and the eigenvaules are assumed not to change sign as $\gamma \to \infty$. Interesting was that we were able to find solutions for negative γ as well. The implicit function theorem only provided existence of solutions but nothing else. Even though we were guaranteed the existence of solutions for all $\gamma < 0$ when $\delta = 1$ we were not able to find a solution for large negative γ and the reason is the increasing norm and the need of a larger domain which was computationaly heavy. The excited states grew even faster in norm for negative γ, which was not very surprising since their L^2-norms are larger than the L^2-norm of the ground state, which made it even harder to find solutions. Our best guess is that higher excieted states will grow even faster, both in norm as well as in domain, for negative γ. No bifurcations were detected either.

When considering negative δ we saw that the norm seemed to explode as $\gamma \to \delta^+$ and trying to compute a solution past this limit resulted in the trivial solution. Interesting is that an eigenvalue seems to tend to 0 as $\gamma \to \delta^+$ but if this is due to a bifurcation or because the computational domain is too small remains unknown. Another observation is that the limit solution as $\gamma \to \delta^+$ seems to have equal shape independent of δ but for negative δ with larger magnitude it becomes harder to compute a solution with γ close to $-\delta$. Also, the second integral identity is far from satisfied here, so we should be careful when drawing any conclusions.

A Mathematical framework

The reader is assumed to be familiar with the mathematical concepts appearing throughout this thesis and the purpose of this appendix is thus merely to avoid possible misunderstandings which may arise from the notation used. For convenience, the main theorems upon which the results of this thesis rely can be found in this appendix as well as a part of the mathematical framework.

A.1 Lebesgue and Sobolev spaces

Definition For $1 \leq p < \infty$, let $\mathcal{L}^p(\mathbb{R}^2)$ be the space of all complex-valued Lebesgue p-integrable functions,

$$\mathcal{L}^p(\mathbb{R}^2) = \{f : \mathbb{R}^2 \to \mathbb{R}, \int_{\mathbb{R}^2} |f|^p \, dx < \infty\}. \tag{A.1}$$

Functions which only differ on a set of measure zero are identified by creating the quotient vector space $L^p = \mathcal{L}^p/\mathcal{N}$ where $\mathcal{N} = \{f \in \mathcal{L}^p : \|f\|_p = 0\}$ where the norm is given by

$$\|f\|_p = \left(\int_{\mathbb{R}^2} |f|^p dx \right)^{\frac{1}{p}}. \tag{A.2}$$

Similarly, we let $L^\infty(\mathbb{R}^2)$ denote the space of essentially bounded complex-valued functions defined on $\mathbb{R}^2$ where two functions are considered equal if they only differ on a set of measure zero.

The space L^2 equipped with the inner-product

$$\langle f, g \rangle = \int_{\mathbb{R}^2} f\overline{g} \, dx \tag{A.3}$$

is a Hilbert space. Special subspaces of the L^p-spaces, Sobolev spaces, consist of those functions whose weak partial derivatives belong to the same space as the differentiated function and they are the foundation of much of the work carried out in this thesis.

Definition For $k \in \mathbb{N}$ the Sobolev space $H^k(\mathbb{R}^2)$ is defined as

$$H^k(\mathbb{R}^2) = \{f \in L^2(\mathbb{R}^2) : \partial^\alpha f \in L^2(\mathbb{R}^2),\ |\alpha| \leq k\} \tag{A.4}$$

where $\partial^\alpha = \partial_{x_1}^{\alpha_1}\partial_{x_2}^{\alpha_2}$ and $|\alpha| = \alpha_1 + \alpha_2$.

The notation $W^{k,2}$ is often seen instead of H^k, which indicates that this is a special case of a more general definition where L^2 is replaced by L^p. The spaces H^k are, as the notation indicates, Hilbert spaces under the inner-product

$$\sum_{|\alpha|\leq k} \int_{\mathbb{R}^2} \partial^\alpha f(x)\overline{\partial^\alpha g(x)}dx \tag{A.5}$$

but the reader should be aware that this thesis uses the slightly different fractional Sobolev spaces defined in the next section. Finally, we need a few theorems helping us to relate the set of Sobolev functions to other spaces of functions such as the continuous ones. Note that the theorems below are special cases adapted to fit the framework in this thesis. For the full general versions the reader is referred to the literature cited in the corresponding proofs.

Theorem A.1 (Sobolev Embedding Theorem) *Let $\dot{C}(\mathbb{R}^2)$ be defined by*

$$\dot{C}(\mathbb{R}^2) = \{f : \mathbb{R}^2 \to \mathbb{R}, f \text{ continuous and } f(x) \to 0 \text{ as } |x| \to \infty\}.$$

Then $H^2(\mathbb{R}^2) \hookrightarrow \dot{C}(\mathbb{R}^2)$ meaning that $H^2(\mathbb{R}^2) \subset \dot{C}(\mathbb{R}^2)$ and the inclusion map is continuous.

Proof See for example [1, Chapter 4].

Theorem A.2 (Sobolev Embedding Theorem)

$$H^1(\mathbb{R}^2) \hookrightarrow L^p(\mathbb{R}^2),\ \forall p \in [2, \infty).$$

Proof See for example [1, Chapter 4].

Theorem A.3 (Rellich-Kondrachov Theorem) *$H^2(\mathbb{R}^2)$ is compactly embedded in $C(\overline{\Omega})$ for any bounded open subset Ω of $\mathbb{R}^2$.*

Proof See for example [1, Chapter 6].

Theorem A.4 *$H^2(\mathbb{R}^2)$ is an algebra under multiplication in the sense that $u, v \in H^2(\mathbb{R}^2) \Rightarrow uv \in H^2(\mathbb{R}^2)$, and there exists a constant $C > 0$ independent of u and v such that*

$$\|uv\|_{H^2(\mathbb{R}^2)} \leq C\|u\|_{H^2(\mathbb{R}^2)}\|v\|_{H^2(\mathbb{R}^2)}.$$

Proof See for example [1, Chapter 4].

A.2 The Fourier transform

Definition For $f \in L^2(\mathbb{R}^2)$ the Fourier transform, $\mathcal{F} : L^2(\mathbb{R}^2) \to L^2(\mathbb{R}^2)$, is defined by

$$\mathcal{F}(f)(\xi) = \hat{f}(\xi) = \frac{1}{2\pi} \int_{\mathbb{R}^2} f(x) e^{-ix\cdot\xi} dx \tag{A.6}$$

for all $\xi \in \mathbb{R}^2$.

Recall that $\mathcal{F}$ is an isomorphism on $L^2(\mathbb{R}^2)$ since it preserves the inner-product

$$\langle \mathcal{F}(f), \mathcal{F}(g) \rangle \;=\; \langle f, \mathcal{F}^{-1}\mathcal{F}(g) \rangle \;=\; \langle f, g \rangle$$

$\forall f, g \in L^2(\mathbb{R}^2)$. The Sobolev space $H^k(\mathbb{R}^2)$ can also be defined using the Fourier transform. First note that there exist constants C_1, C_2 such that $C_1(1+|\xi|^2)^k \leq \sum_{|\alpha|\leq k} \xi^{2\alpha} \leq C_2(1+|\xi|^2)^k$ for each $\xi \in \mathbb{R}^2$. By interchanging the sum and integral in (A.5) and applying the Fourier transform we get

$$\sum_{|\alpha|\leq k} \int_{\mathbb{R}^2} \partial^\alpha f(x) \overline{\partial^\alpha g(x)} dx = \int_{\mathbb{R}^2} \sum_{|\alpha|\leq k} \xi^{2\alpha} |\hat{f(\xi)}|^2 d\xi < \infty \tag{A.7}$$

and therefore $f \in L^2(\mathbb{R}^2)$ belongs to $H^k(\mathbb{R}^2)$ if and only if

$$\|f\|^2_{H^k(\mathbb{R}^2)} = \int_{\mathbb{R}^2} (1+|\xi|^2)^k |\hat{f}(\xi)|^2 d\xi < \infty \tag{A.8}$$

which, unlike (A.7), is well-defined for any real k. Thus, we can introduce the extended family of (fractional) Sobolev spaces, $H^s(\mathbb{R}^2)$ where $s \in \mathbb{R}$, defined by

$$H^s(\mathbb{R}^2) = \{ f \in L^2(\mathbb{R}^2) : (1+|\xi|^2)^{s/2} \hat{f}(\xi) \in L^2(\mathbb{R}^2) \} \tag{A.9}$$

equipped with a norm defined by the integral in (A.8) with k replaced by s.

Theorem A.5 *The map $-\Delta + I : H^2(\mathbb{R}^2) \to L^2(\mathbb{R}^2)$ is an isometric isomorphism.*

Proof $-\Delta + I$ is surjective since for any $g \in L^2(\mathbb{R}^2)$ the function f defined by $\hat{f} = \frac{\hat{g}}{|\xi|^2+1}$ satisfies $(-\Delta+I)f = g$ and by (A.9) it is clear that $f \in H^2(\mathbb{R}^2)$. The isometry property follows from the observation,

$$\|(-\Delta+I)f\|_{L^2(\mathbb{R}^2)} = \|\mathcal{F}((-\Delta+I)f)\|_{L^2(\mathbb{R}^2)} =$$
$$\|(1+|\xi|^2)|\hat{f}|\|_{L^2(\mathbb{R}^2)} = \|f\|_{H^2(\mathbb{R}^2)}.$$

A.3 Operator theory

Let X and Y be Banach spaces and let T be a linear operator

$$T : \mathcal{D}(T) \subseteq X \to Y \tag{A.10}$$

where the domain of T, $\mathcal{D}(T)$, is a linear subspace of X. We will denote the null-space and the range of T by $\mathcal{N}(T)$ and $\mathcal{R}(T)$ respectively.

Definition Let T be a linear operator defined on $\mathcal{D}(T)$ as above. If $\mathcal{D}(T)$ is dense in X, we say that the operator T is densely defined.

Throughout this thesis, all linear operators are assumed to be densely defined. In particular, for a bounded linear operator T, the domain of T is assumed to be equal to the whole space X since T can be extended uniquely by continuity to a linear operator with domain $\overline{\mathcal{D}(T)} = X$.

Definition Let X, Y be Banach spaces. We denote by $\mathcal{L}(X, Y)$ the space of all continuous linear operators from X to Y. In particular, if $X = Y$, we write $\mathcal{L}(X) = \mathcal{L}(X, X)$.

We can use linear operators to define what it means to differentiate an operator, whenever this is possible.

Definition (Fréchet derivative) Let F be an operator between Banach spaces X and Y and let $U \subset X$ be open. Then F is said to be differentiable at $x \in U$ (in the sense of Fréchet) if there exists a linear map $T \in \mathcal{L}(X, Y)$ such that

$$F(x + v) = F(x) + T(v) + R(v) \tag{A.11}$$

where $\frac{\|R(v)\|_Y}{\|v\|_X} \to 0$ as $\|v\|_X \to 0$.

The map T, often denoted $dF(x)$ or $D_x F$, is called the Fréchet-derivative of F at x and is, if it exists, unique [2]. We can also define partial derivatives of an operator.

Definition (Partial Fréchet derivatives) Suppose that X, Y and Z are Banach spaces, that $U \subset X \times Y$ is open and $F : U \to Z$. Suppose that $(x_0, y_0) \in U$. Then $U_{x_0} = \{y \in Y : (x_0, y) \in U\}$ is open. If the function $F(\cdot, y_0)$ has a Fréchet derivative at x_0 we denote it by $F_x(x_0, y_0) \in \mathcal{L}(X, Z)$ and refer to it as the partial Fréchet derivative of F with respect to x at (x_0, y_0). Similarly $F_y(x_0, y_0) : Y \to Z$ will denote the partial Fréchet derivative of F with respect to y.

The next theorems are central in this thesis since they allow us to deduce the existence of solutions to the DS equation.

Theorem A.6 (Implicit Function Theorem) *Let $F \in C^k(\Lambda \times U, Y), k \geq 1$, where Y is a Banach space and Λ (resp. U) is an open subset of Banach space Z (resp. X). Suppose that $F(\lambda^*, u^*) = 0$ and that $F_u(\lambda^*, u^*)$ is invertible.*

Then there exist neighbourhoods Θ of λ^* in Z and U^* of u^* in X and a map $g \in C^k(\Theta, X)$ such that

- *$F(\lambda, g(\lambda)) = 0$ for all $\lambda \in \Theta$,*
- *$F(\lambda, u) = 0, (\lambda, u) \in \Theta \times U^*$, implies $u = g(\lambda)$,*
- *$g'(\lambda) = -[F_u(p)]^{-1} \circ F_\lambda(p)$, where $p = (\lambda, g(\lambda))$ and $\lambda \in \Theta$.*

Proof See for example [2, p.38].

Definition Let X be a Banach space. For a linear operator $T : \mathcal{D}(T) \subseteq X \to X$ the resolvent set of T is defined by

$$\rho(T) = \{\lambda \in \mathbb{C} : (T - \lambda I)^{-1} \text{ exists and is bounded}\} \tag{A.12}$$

and the complement $\sigma(T)$ is defined as the spectrum of T. The resolvent of T is a function on $\rho(T)$ defined by $R_T(\lambda) = (T - \lambda I)^{-1}$.

There are several ways of classifying the elements in the spectrum and here we will use the definition given by Hislop and Sigal [10].

Definition The point spectrum of T, denoted as $\sigma_p(T)$, is the set of all eigenvalues of T with finite algebraic multiplicity and which also are isolated points points of $\sigma(T)$. The essential spectrum of T is then defined by $\sigma_{ess}(T) = \sigma(T) \setminus \sigma_p(T)$.

Definition An operator $T : \mathcal{D}(T) \subseteq X \to X$ is closed if for every sequence $\{x_n\} \in \mathcal{D}(T)$ such that $x_n \to x$ and $Tx_n \to y$ in X it holds that $x \in \mathcal{D}(T)$ and $y = Tx$.

Definition Let A be an operator on a Hilbert space $\mathcal{H}$ with domain $\mathcal{D}(A)$. The adjoint of A, A^*, is defined on the domain

$$\begin{aligned}\mathcal{D}(A^*) = &\{x \in \mathcal{H} : |\langle Ay, x\rangle| \leq C_x \|y\| \\ &\text{for some constant } C_x \text{ and all } \ y \in \mathcal{D}(A)\}\end{aligned}$$

as the map $A^* : \mathcal{D}(A^*) \to \mathcal{H}$ satisfying $\langle Ay, x\rangle = \langle y, A^*x\rangle$ for all $y \in \mathcal{D}(A)$ and $x \in \mathcal{D}(A^*)$. A is called self-adjoint if $A = A^*$.

It is easily seen that a self-adjoint operator is closed.

Definition An operator A on $\mathcal{H}$ with domain $\mathcal{D}(A)$ is called symmetric if A^* is an extension of A or, equivalently, if $\langle Ax, y\rangle = \langle x, Ay\rangle$ for all $x, y \in \mathcal{D}(A)$.

For the last part of this Appendix we will only consider self-adjoint operators on a Hilbert space $\mathcal{H}$. The purpose of this remainder is to give some definitions enabling us to make sense of and apply Weyl's theorem which helps us find the essential spectrum of certain operators occurring in the thesis. Moreover, we recall some results which can be used to locate the eigenvalues below the essential spectrum.

Definition Let A be a closed operator on $\mathcal{H}$ with domain $\mathcal{D}(A)$ such that $\rho(A) \neq \emptyset$. An operator B is called relatively A-compact if

- $\mathcal{D}(A) \subset \mathcal{D}(B)$ and
- $BR_A(z)$ is compact for at least one (and hence all) $z \in \rho(A)$.

Theorem A.7 *Suppose A is a self-adjoint operator on $\mathcal{H}$ and B is symmetric and relatively A-compact. Then $A + B$ with domain $\mathcal{D}(A)$ is self-adjoint on $\mathcal{H}$.*

Proof See for example Hislop and Sigal [10, p.141].

Theorem A.8 (Weyl's Theorem) *Let A and B be self-adjoint operators on $\mathcal{H}$ and let $A - B$ be relatively A-compact. Then*

$$\sigma_{ess}(A) = \sigma_{ess}(B) \tag{A.13}$$

Proof See for example Hislop and Sigal [10, p.142].

Suppose now that A is a self-adjoint operator on a Hilbert space $\mathcal{H}$. Recall that the Rayleigh quotient corresponding to A is defined by

$$\frac{\langle Ax, x\rangle}{\|x\|^2}, \quad x \in \mathcal{D}(A),$$

and that $\inf \sigma(A) = \inf_{x\in\mathcal{D}(A)} \frac{\langle Ax,x\rangle}{\|x\|^2}$ (see e.g. [22]). A is said to be bounded from below if $\inf \sigma(A) > -\infty$. If A is bounded from below, then there is at most countably many eigenvalues below the essential spectrum, which can be ordered in increasing order: $\lambda_1 \leq \lambda_2 \leq \cdots$ (repeated according to multiplicity). The following min-max theorem gives a way of computing the nth eigenvalue.

Theorem A.9 *Let A be a self-adjoint operator and let $\lambda_1 \leq \lambda_2 \leq \cdots$ be the eigenvalues of A below the essential spectrum. Then*

$$\lambda_n = \max_{x_1,\ldots,x_{n-1}\in\mathcal{H}} \inf_{\mathcal{D}(A)\ni x\perp\{x_1,x_2,\ldots,x_{n-1}\}} \frac{\langle Ax, x\rangle}{\|x\|^2}.$$

Proof See for example Teschl [22, p.141].

Bibliography

[1] Adams, R. A., and Fournier, J. J. F. *Sobolev spaces*, second ed., vol. 140 of *Pure and Applied Mathematics (Amsterdam)*. Elsevier/Academic Press, Amsterdam, 2003.

[2] Ambrosetti, A., and Prodi, G. *A primer of nonlinear analysis*, vol. 34 of *Cambridge Studies in Advanced Mathematics*. Cambridge University Press, Cambridge, 1993.

[3] Benney, D. J., and Roskes, G. J. Wave instabilities. *Studies in Applied Mathematics 48*, 4 (1969), 377–385.

[4] Chang, S.-M., Gustafson, S., Nakanishi, K., and Tsai, T.-P. Spectra of linearized operators for NLS solitary waves. *SIAM J. Math. Anal. 39*, 4 (2007/08), 1070–1111.

[5] Cipolatti, R. On the existence of standing waves for a Davey-Stewartson system. *Comm. Partial Differential Equations 17*, 5-6 (1992), 967–988.

[6] Cortázar, C., García-Huidobro, M., and Yarur, C. S. On the uniqueness of sign changing bound state solutions of a semilinear equation. *Ann. Inst. H. Poincaré Anal. Non Linéaire 28*, 4 (2011), 599–621.

[7] Davey, A., and Stewartson, K. On three-dimensional packets of surface waves. *Proc. Roy. Soc. London Ser. A 338* (1974), 101–110.

[8] Djordjević, V. D., and Redekopp, L. G. On two-dimensional packets of capillary-gravity waves. *J. Fluid Mech. 79*, 4 (1977), 703–714.

[9] Eden, A., and Topaloglu, I. A. Standing waves for a generalized Davey-Stewartson system: revisited. *Appl. Math. Lett. 21*, 4 (2008), 342–347.

[10] Hislop, P. D., and Sigal, I. M. *Introduction to spectral theory*, vol. 113 of *Applied Mathematical Sciences*. Springer-Verlag, New York, 1996. With applications to Schrödinger operators.

[11] Iaia, J., and Warchall, H. Nonradial solutions of a semilinear elliptic equation in two dimensions. *J. Differential Equations 119*, 2 (1995), 533–558.

[12] Jones, C., and Küpper, T. On the infinitely many solutions of a semilinear elliptic equation. *SIAM J. Math. Anal. 17*, 4 (1986), 803–835.

[13] Kim, B., and Akylas, T. R. On gravity-capillary lumps. *J. Fluid Mech. 540* (2005), 337–351.

[14] Kim, B., and Akylas, T. R. On gravity-capillary lumps. II. Two-dimensional Benjamin equation. *J. Fluid Mech. 557* (2006), 237–256.

[15] Kwong, M. K. Uniqueness of positive solutions of $\Delta u - u + u^p = 0$ in $\mathbf{R}^n$. *Arch. Rational Mech. Anal. 105*, 3 (1989), 243–266.

[16] Lions, P.-L. Solutions complexes d'équations elliptiques semilinéaires dans $\mathbf{R}^N$. *C. R. Acad. Sci. Paris Sér. I Math. 302*, 19 (1986), 673–676.

[17] McLeod, K., Troy, W. C., and Weissler, F. B. Radial solutions of $\Delta u + f(u) = 0$ with prescribed numbers of zeros. *J. Differential Equations 83*, 2 (1990), 368–378.

[18] Milewski, P. A., and Wang, Z. Three dimensional flexural-gravity waves. *Stud. Appl. Math. 131*, 2 (2013), 135–148.

[19] Papanicolaou, G. C., Sulem, C., Sulem, P.-L., and Wang, X. P. The focusing singularity of the Davey-Stewartson equations for gravity-capillary surface waves. *Phys. D 72*, 1-2 (1994), 61–86.

[20] Renardy, M., and Rogers, R. C. *An introduction to partial differential equations*, second ed., vol. 13 of *Texts in Applied Mathematics*. Springer-Verlag, New York, 2004.

[21] Seydel, R. *Practical bifurcation and stability analysis*, third ed., vol. 5 of *Interdisciplinary Applied Mathematics*. Springer, New York, 2010.

[22] Teschl, G. *Mathematical methods in quantum mechanics*, second ed., vol. 157 of *Graduate Studies in Mathematics*. American Mathematical Society, Providence, RI, 2014.

[23] Trefethen, L. N. *Spectral methods in MATLAB*, vol. 10 of *Software, Environments, and Tools*. Society for Industrial and Applied Mathematics (SIAM), Philadelphia, PA, 2000.

[24] Yang, J. Newton-conjugate-gradient methods for solitary wave computations. *J. Comput. Phys. 228*, 18 (2009), 7007–7024.

[25] Yang, J. *Nonlinear waves in integrable and nonintegrable systems*, vol. 16 of *Mathematical Modeling and Computation*. Society for Industrial and Applied Mathematics (SIAM), Philadelphia, PA, 2010.

[26] Zettl, A. *Sturm-Liouville theory*, vol. 121 of *Mathematical Surveys and Monographs*. American Mathematical Society, Providence, RI, 2005.

Master's Theses in Mathematical Sciences 2016:E14
ISSN 1404-6342

LUNFMA-3089-2016

Mathematics
Centre for Mathematical Sciences
Lund University
Box 118, SE-221 00 Lund, Sweden

http://www.maths.lth.se/